

EVALUATING FLEXIBLE PAVEMENT RUT DAMAGE CAUSED BY MULTIPLE AXLE AND TRUCK CONFIGURATIONS

Hassan Salama and Karim Chatti

Michigan State University

Karim Chatti

Associate Professor

Department of Civil and Environmental Engineering,
3546 Engineering Building, Michigan State University, East Lansing, Michigan 48824
517-355-6534
chatti@egr.msu.edu

ABSTRACT

In this paper, the effect of trucks with multiple axle configurations on flexible pavement rutting is investigated using a mechanistic-empirical rut model that takes into account the rutting contributions from the various layers comprising the pavement structure and in the laboratory. Five different axle types (single, tandem, tridem, quad, and 8-axle) and five truck configurations (two five-axle and three eleven-axle trucks) were analyzed. The mechanistic analysis indicates that there is little to no interaction between axles in the vertical strain response within the upper layers, and this interaction increases with depth to become significant within the subgrade layer. Despite the interaction between axles in the lower pavement layers, the mechanistic analysis still showed that rutting is proportional to the gross vehicle weight if the entire strain pulse is used in the calculation. The laboratory results show that rutting in the asphalt concrete is nearly proportional to the number of axles within an axle group, with larger axle groups causing slightly less rut damage per load carried. There was more variation in the results from different truck configurations, although trucks with larger axle configurations still showed less damage per load carried. The laboratory results also indicate that smaller rest periods between axle groups within a given truck configuration have led to more rut damage per load carried as compared to the equivalent number of individual axle loads.

EVALUATING FLEXIBLE PAVEMENT RUT DAMAGE CAUSED BY MULTIPLE AXLE AND TRUCK CONFIGURATIONS

Hassan Salama¹ and Karim Chatti²

¹ Research Associate, e-mail: salamaha@egr.msu.edu

² Associate Professor, email: chatti@egr.msu.edu, phone: 517-355-6534; fax: 517-432-1827
Department of Civil and Environmental Engineering, 3546 Engineering Building,
Michigan State University, East Lansing, Michigan 48824

1 BACKGROUND

Since rutting is a major failure mode in flexible pavements, researchers have been trying to predict rut depth for future rehabilitation and budget allocation. There are two main approaches for the prediction of rutting: the first approach assumes that most of the rutting results from the subgrade layer only, and is no longer valid based on observations from the field. The two most widely used equations related to the subgrade strain model are the Asphalt Institute (AI) model (Shook *et al.*, 1982) and the Shell Petroleum model (Claussen *et al.*, 1977). The second approach considers the rutting contribution from all pavement layers, and is not widely used due to the difficulties in determining the elasto-plastic characteristics of pavement materials. However, this approach has been adopted in the newly proposed mechanistic-empirical (ME) pavement design guide for the U.S. (Witczak and El-Basyouny, 2004.)

One of the main models related to this approach is the VESYS rutting model that relates the plastic strain to the elastic strain through the permanent deformation parameters (PDPs) μ and α as follows:

$$\varepsilon_p(n) = \mu * \varepsilon_e * n^{-\alpha} \quad (1)$$

The VESYS rutting model (Moavenzadeh *et al.*, 1974) was derived so that each term of the equation corresponds to one pavement layer with two unique permanent deformation parameters (α and μ). The form of the model is more applicable for use in mechanistic-empirical design (Ali *et al.*, 1998, Ali and Tayabji, 2000). The most essential task in using this model is to accurately determine PDPs (α and μ) for each pavement layer within the pavement system. Several attempts have been made to estimate these parameters; however agreement between studies varies, providing a common but wide range for these parameters. As can be seen in Equation 1, α is an exponent and therefore prediction of rutting is very sensitive to it. Equation 2 shows the VESYS rutting model for a three-layer pavement system (asphalt concrete, base and subgrade).

$$\rho_p = h_{AC} \frac{\mu_{AC}}{1-\alpha_{AC}} \left(\sum_{i=1}^K (n_i)^{1-\alpha_{AC}} (\varepsilon_{ei,AC}) \right) + h_{base} \frac{\mu_{base}}{1-\alpha_{base}} \left(\sum_{i=1}^K (n_i)^{1-\alpha_{base}} (\varepsilon_{ei,base}) \right) + h_{SG} \frac{\mu_{SG}}{1-\alpha_{SG}} \left(\sum_{i=1}^K (n_i)^{1-\alpha_{SG}} (\varepsilon_{ei,SG}) \right) \quad (2)$$

where:

- ρ_p = Total cumulative rut depth (mm),
 i = Subscript indicating axle group,
 K = Number of axle groups,
 h = Layer thickness for AC, combined base and subgrade layers, respectively (mm),
 n = Number of load applications,
 ε_e = Compressive vertical elastic strain at the middle of the layers,
 μ = Constant of proportionality between plastic and elastic strain, and
 α = Constant indicating the rate of rutting decrease as the number of load applications increases.

In this paper, the effect of trucks with multiple axle configurations on flexible pavement rutting is investigated using a mechanistic-empirical rut model that takes into account the rutting contributions from the various layers comprising the pavement structure and in the laboratory.

2 CALIBRATED MECHANISTIC-EMPIRICAL RUTTING MODEL

Salama et al. (2006) backcalculated the PDPs by matching the rut time series data from the SPS-1 experiment in the LTPP program. The most novel aspect of this backcalculation process involved the application of the approach developed in NCHRP 468 (White *et al.*, 2002), which uses transverse surface profiles to locate the layer causing most of the rutting. Using this process, the most likely solution for these parameters was obtained for 109 pavement sections within the SPS-1 experiment. The backcalculated PDPs were then used in multivariate regression analyses to develop models for predicting α and μ for a three-layer pavement system (asphalt concrete, base and subgrade). All available material, structural and climatic data used to explain rutting were extracted from the LTPP database for those 109 pavement sections. Using simple linear regression, α and μ were regressed against these independent variables. The variables that have reasonable relationships (relatively higher R^2) were introduced into the multiple linear regression models. The backward regression analysis was used to select the statistically significant variables for the final models. Because limited material data availability in the LTPP database, only 15 out of 109 sections were used for predicting α_{AC} and μ_{AC} ; 27 sections were used for predicting α_{base} and μ_{base} ; and 17 sections were used for predicting $\alpha_{subgrade}$ and $\mu_{subgrade}$ (Salama et al., 2006). Equations 3 to 8 show the PDPs prediction equations for AC (HMA), base, and subgrade layers.

$$\alpha_{HMA} = 5105.124 * (\text{Strain})^{0.555} * P_{10}^{-1.013} * (VFA)^{-0.58} * (MAAT)^{0.732} \quad (3)$$

$$\mu_{HMA} = 6.746 * \alpha_{AC}^{4.102} * FI^{-0.213} \quad (4)$$

where:

- Strain = Strain in the middle of AC layer due to one standard axle,
 P_{10} = % passing sieve number 10 of the most upper AC layer,
 VFA = % voids filled with asphalt of the most upper AC layer,
 $MAAT$ = Average of daily maximum air temperatures for year ($^{\circ}\text{C}$),
 FI = Freezing index.

$$\alpha_{base} = 2.724 * 10^{-5} * \text{modulus}^{0.102} * \text{Thickness}^{0.066} * P_{200}^{-0.098} * GI^{1.982} \quad (5)$$

$$\mu_{base} = 7.1977 * 10^{-3} * \alpha_{base}^{6.256} * \text{Thickness}^{-0.808} * \text{strain}^{-0.809} \quad (6)$$

where:

- modulus = Backcalculated base modulus (psi),
- Thickness = Thickness of base layer used in the backcalculation (mm),
- P₂₀₀ = % passing sieve number 200,
- GI = Gradation index (as calculated from Equation 9),
- strain = Strain in the middle of the base layer due to one standard axle.

$$\alpha_{SG} = 1.385 \times 10^{-5} * strain^{0.043} * GI^{1.89} * PI^{0.116} * D_{32}^{0.14} * FI^{0.036} * wet\ days^{0.326} \quad (7)$$

$$\mu_{SG} = 2.575 * 10^{-63} * modulus^{2.41} * strain^{-0.764} * GI^{22.594} * PI^{1.304} \quad (8)$$

where:

- Strain = Strain in the middle of the first 1016 mm of subgrade due to one standard axle,
- GI = Gradation index (as calculated from Equation 9),
- PI = Plasticity index of subgrade layer,
- D₃₂ = Number of days per year with daily maximum air temperature above 32.2 °C,
- Wet days = Number of days per year with precipitation greater than 0.25 mm,
- Modulus = Backcalculated subgrade modulus (psi).






$$GI = \frac{\sum p * \log SS}{\sum \log SS} \quad (9)$$

where: p = % passing of the individual sieve, and $\log SS$ = logarithm of sieve size in mm.

3 ANALYSIS

The main objective of this paper is to apply the calibrated mechanistic-empirical rutting model to compare the relative rutting damage due to different axle and truck configurations (Table 1). The selection of pavement profiles in this study was designed to examine the effect of heavy axle trucks on a thick pavement, where there is interaction in the base and subgrade layers, and a thin pavement, where there is interaction in the subgrade layer only. Table 2 shows the layer thicknesses and moduli of the two pavement cross-sections used in the analysis. Section 1 is hypothetical and represents a thick pavement, while section 2 is from the SPS-1 experiment and represents a thin pavement. The layer moduli for the SPS-1 section were backcalculated using the MICHBACK computer program (Harichandran *et al.*, 1994).

Table 1. Axle and truck configurations used in the analysis.

Variable	Axle and truck configurations				
	(1)	(2)	(3)	(4)	(5)
Axles	Single	Tandem	Tridem	Quad	8-axles
Trucks*	S ₅ ** 	S ₁ T ₂ 	S ₁ T ₂ Tr ₂ 	S ₃ T ₂ Q ₁ 	S ₁ T ₁ E ₁ ** 

* Trucks defined by their axle configuration

** S₅ = Truck with five single axles; S₁T₁E₁ = truck with one single axle + one tandem axle + one eight axle

Table 2. Pavement cross-sections and moduli.

Cross-section #	AC		Base		Subgrade
	Thickness, mm	Modulus, psi*	Thickness, mm	Modulus, psi	Modulus, psi
1	203	450000	914	30000	10000
2**	104	551236	208	55283	23205

* 1 psi = 6.89 kPa

** Section 50113 from the SPS-1 experiment (LTPP database)

3.1 Calculating strain pulses under multiple axles

Since there is no available software that can handle larger than tridem axle groups, the KENLAYER (Huang, 1993) layered elastic analysis program was used with responses due to larger axle groups being calculated by superposition. As shown in Figure 1, the vertical compressive elastic strain (VCES) due to multiple axles at the middle of the AC, base, and six 40 inch (1,016-mm) subsequent layers of subgrade were calculated. The standard axle load used in this analysis is 18 kips (80.07 kN) with a tire pressure of 70 psi (482.63 kPa), while the single axle load is 13 kips (57.83 kN) with a tire pressure of 100 psi (689.48 kPa). The responses due to different multiple axle and truck configurations were compiled from the superposition of the appropriate number and spacing of single axles. As an example, Figures 2 and 3 show the VCES at the middle of the AC, base, and top subgrade (SG) layers due to an 8-axle group for cross-sections 1 and 2. Since the VCES curve flattens and widens as the depth within the subgrade increases, only the top subgrade layer is depicted; however, all subgrade layers were considered in the calculation.

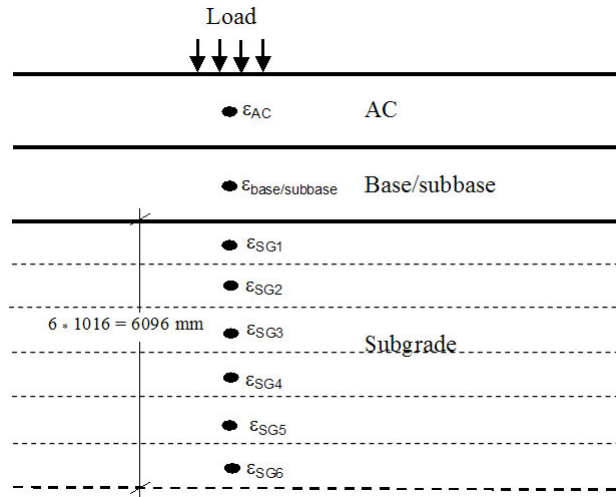


Figure 1. Division of the subgrade layer into several sub-layers.

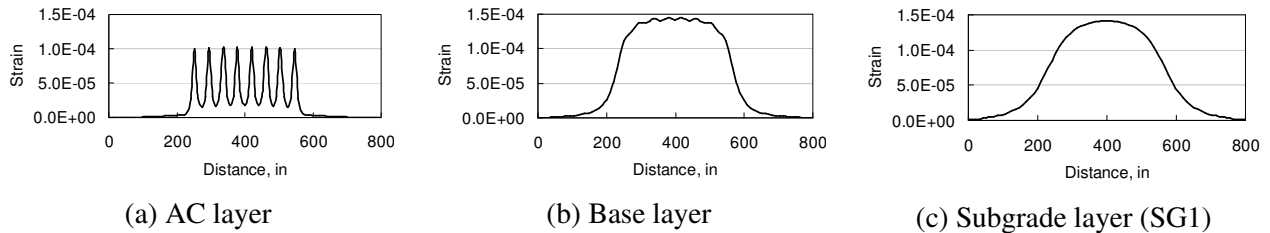


Figure 2. Vertical strain pulses due to 8-axle group on thick pavement (section 1).

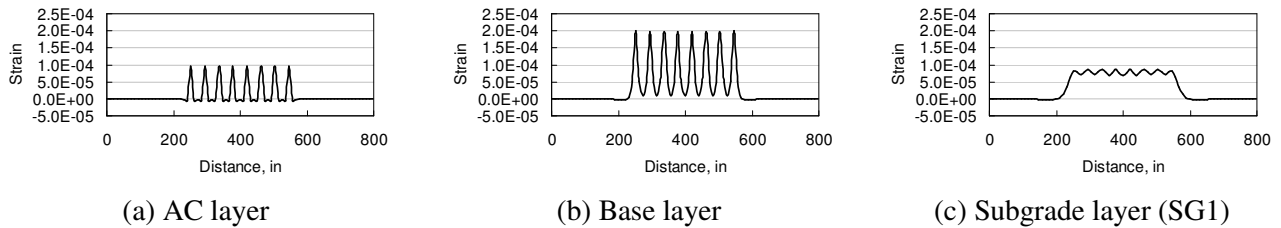


Figure 3. Vertical strain pulses due to 8-axle group on thin pavement (section 2).

3.2 Calculating rut damage caused by multiple axles

The calibrated mechanistic-empirical rutting model makes it possible to mechanistically compare the rut damage due to different axle and truck configurations for specific pavement sections. The PDPs for the two cross-sections were calculated from the developed regression equations (3 to 8). It should be noted that the pavement layer thicknesses and moduli shown in Table 2 were inputs for these equations, whereas all other variables were assumed at the mean values of the range used to develop the regression equations (Salama, 2005). Table 3 shows the calculated PDPs for these cross-sections.

Table 3. Calculated PDPs.

	α_{AC}	μ_{AC}	α_{base}	μ_{base}	α_{SG}	μ_{SG}
Cross-Section 1	0.702	0.537	0.741	0.134	0.873	0.010
Cross-Section 2	0.594	0.271	0.716	0.129	0.910	0.037

As shown in Figures 2 and 3, the 8-axle responses (VCES) in the middle of the AC layer have lower interaction levels, and the interaction level increases with depth until the 8-axle response becomes one, wide pulse at deeper sub-layers. To study the effect of the strain pulse duration and the interaction on rutting calculation for different axle and truck configurations, two different procedures were used: 1) sum the rutting damage due to only the strain values underneath each axle within an axle group, and 2) sum the rutting damage due to the strain values underneath the axles (procedure 1) as well as those outside the axle group (at consistent intervals) until the strain becomes negligible. The reasoning behind the second procedure is that the entire strain influence curve should be considered since it defines the total response due to the event of an axle group or a truck passing over a given point in the pavement. A diagram illustrating these two procedures for calculating rut damage due to an 8-axle group is shown in Figure 4. The rutting due to one million repetitions of different axle and truck configurations were calculated using both procedures for each layer for both cross-sections. The results are presented next.

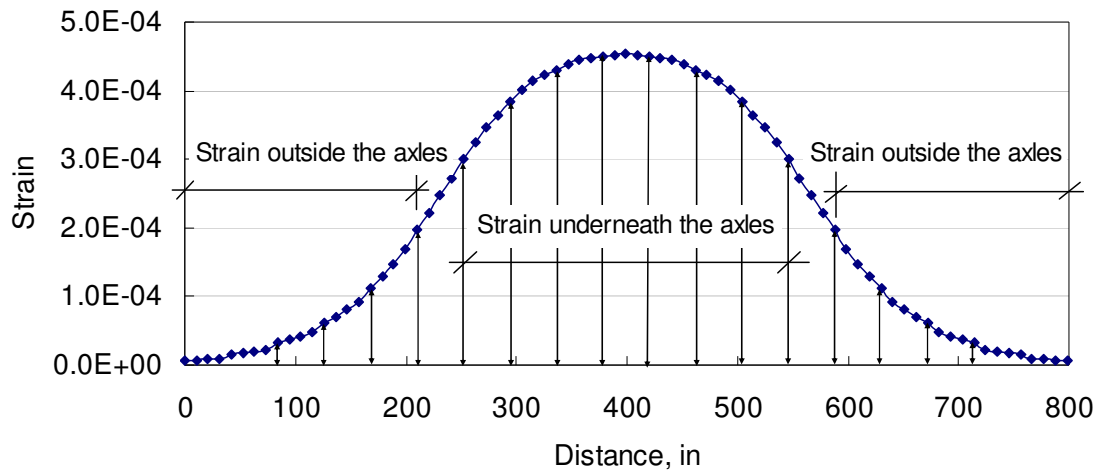


Figure 4. Strain influence curve under an 8-axle group.
(1 inch = 25.4 mm)

3.3 Results

The rut depth for individual layers and the total rut depth due to one million repetitions of different axle and truck configurations were calculated for pavement sections 1 and 2 using both

procedures. The results were normalized to the rut depth caused by a single axle to study the relative effect of different axle and truck configurations on pavement rut damage, and are shown in Figures 5 through 8 in terms of ‘axle factors’ (AF) and ‘truck factors’ (TF), as defined below:

$$AF = \frac{\text{Rut depth due to a given axle group}}{\text{Rut depth due to a single axle}} \quad (10)$$

$$TF = \frac{\text{Rut depth due to a given truck}}{\text{Rut depth due to a single axle}} \quad (11)$$

The results show that when there is no strain interaction between axles, both procedures for calculating the rut depth show rutting damage proportional to the number of axles. This is the case for AC layer of cross-section 1 and AC and base layers of cross-section 2. On the other hand, when there is strain interaction between the axles, the first procedure (accounting only for the strain values under the axles) would lead to the conclusion that multiple axles are more damaging relative to the same number of single axles (Figures 5 and 6). This result is due to the fact that procedure 1 ignores the strains outside the axles and the effect of these strain values becomes more important at higher levels of interaction. However, since these strain values do result in rutting damage, it is not logical to ignore them. Calculating the rut depth by accounting for all strain values (strain underneath and outside the axles) shows that whether there is strain interaction or not, the axle and truck factors are proportional to the number of axles (Figures 7 and 8). This is to be expected since: (1) using the entire strain influence curve would give the total response of the pavement system; (2) the analysis assumes linear elastic response; and (3) the VESYS model assumes that the plastic strain is proportional to the elastic strain. This suggests that procedure 2 should be favored over procedure 1 when calculating the rut depth due to multiple axle and truck configurations using mechanistic analysis.

In a similar mechanistic analysis of the effect of heavy-vehicle characteristics on pavement response and performance using a viscoelastic layered response model, Gillespie *et al.* (1993) calculated the rut depth for different truck configurations by integrating the influence function due to a moving load, which resulted in rutting damage that is proportional to the axle load.

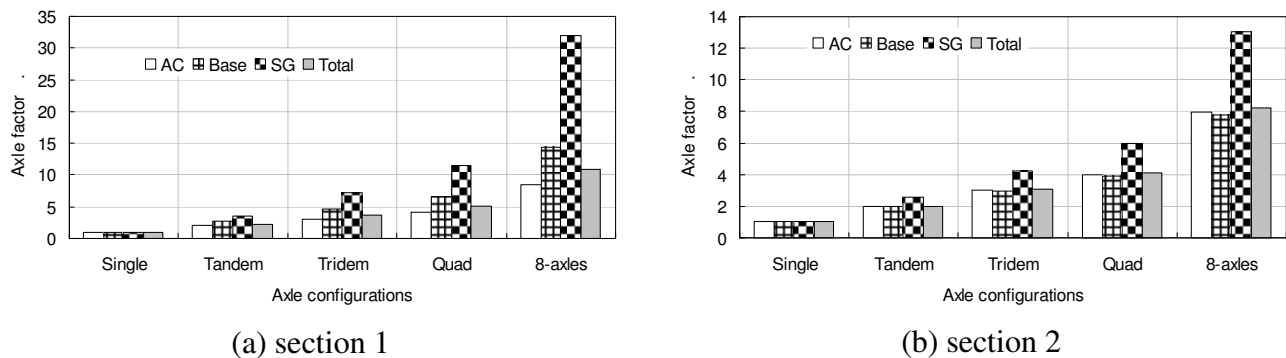
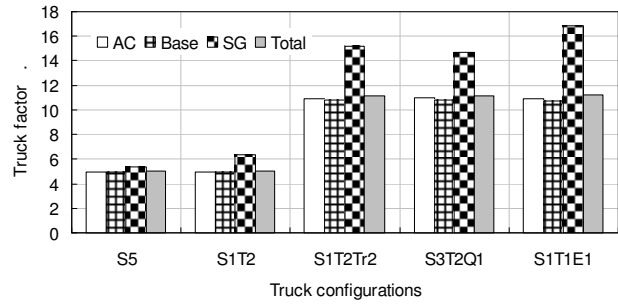
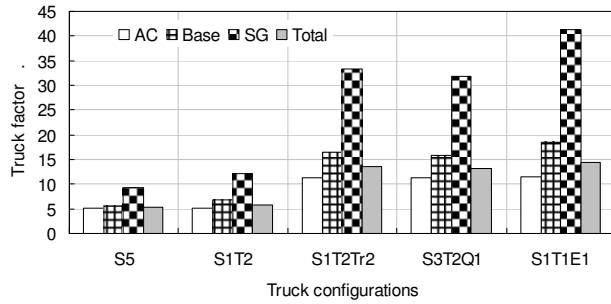


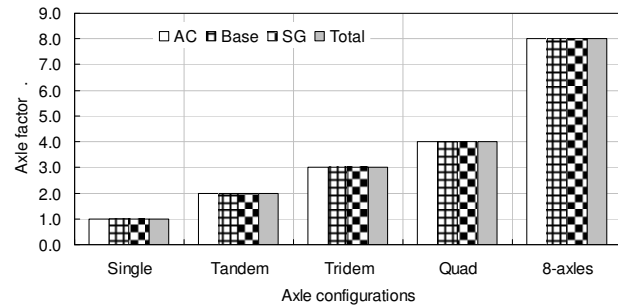
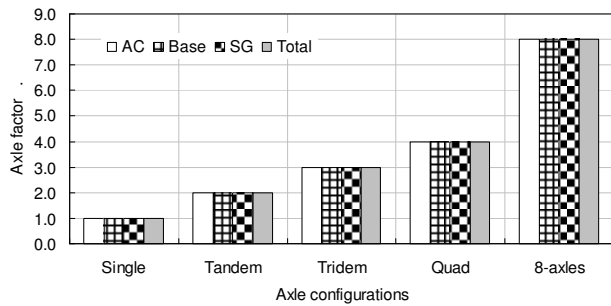
Figure 5. Axle factors – procedure 1.



(a) section 1

(b) section 2

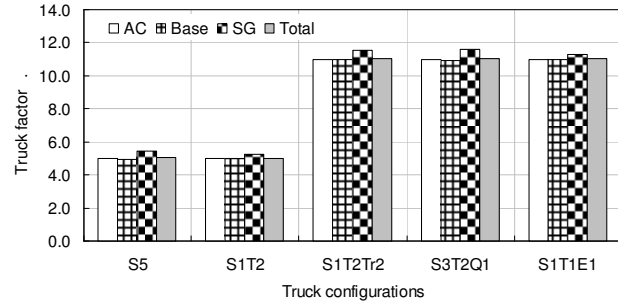
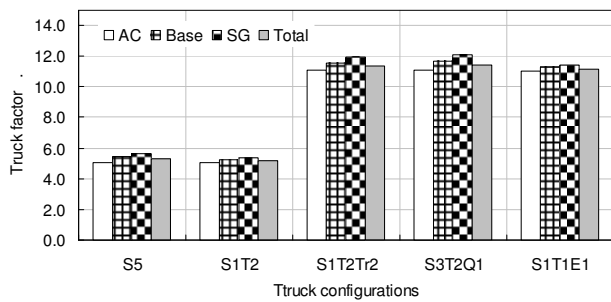
Figure 6. Truck factors – procedure 1.



(a) section 1

(b) section 2

Figure 7. Axle factors – procedure 2.



(a) section 1

(b) section 2

Figure 8. Truck factors – procedure 2.

4 LABORATORY RESULTS

The same axles and trucks used in the mechanistic analysis (Table 1) were simulated in the laboratory using multiple pulse loadings. The samples used in this laboratory experiment were prepared according to the new simple performance testing (SPT) procedure (Witczak *et al.*, 2002). A uniform asphalt concrete mix (4E3-MDOT) was used to produce cylinders that are 3.7 in (94 mm) in diameter and 6 in (152mm) in height with an average air void content of 4.22% after coring. The unconfined cyclic compression load tests were conducted using an MTS electro-hydraulic test machine at a controlled temperature of 100°F ($\pm 1^\circ\text{F}$) and at three stress levels. The samples were gradually heated inside the test chamber over the course of 12 hours

before starting the actual test to insure uniform temperature throughout the mass of the specimen. Two steel plates (one at the top and another at the bottom) were used to distribute the load evenly over the cross-sectional area of the specimen. Two linear variable displacement transducers (LVDTs) were placed on the sample to measure vertical deformation. The specimens were subjected to cyclic haversine pulses. The series of cyclic uniaxial compression tests were conducted using different multiple load pulses. The pulses were designed to simulate different axle/truck configurations. The ratio of loading/unloading duration to rest period was held constant at a 1:9 ratio. For single axles, the loading duration was found to be 0.08 s to simulate a load moving at 30 mph; therefore a rest period of 0.72 s was used. For multiple axle and truck configurations, the loading time was taken as the time corresponding to the response due to the first axle until the time when the response due to the last axle dies out. The samples took from 4 to 5 hours until total failure at high stress level for all axle and truck configurations, 9 to 11 hours at medium stress level, and 45 to 50 hours at low stress level.

Figure 9 shows the laboratory-derived axle factors (defined as the ratio of the flow number corresponding to a single axle to that of the axle group in question). The figure indicates that rutting damage in asphalt concrete due to different axle configurations is approximately proportional to the number of axles within an axle group, although the damage caused by larger axle groups appears to be slightly lower per load carried. Figure 10 shows the truck factors for the five truck configurations. The results show more variations, with the truck factors for the five-axle truck ranging from 6 (S1T2 truck) to 8 (S5 truck), and those of the 11-axle trucks from 10 (S1T1E1 truck) to about 14 (S1T2Tr2 and S3T2Q1 trucks). These variations may be partly explained by the following reasons: (i) The rest period between axles within a given truck configuration is not the same as that for the individually tested axles; (ii) the sequence of axles varies from one truck configuration to another. However, the results do indicate that grouping of axles resulted in reduced damage per load carried. The 5-axle trucks with two tandem axles (S1T2) produced less damage than the truck with only single axles (S5). Also, the truck with the 8-axle group (S1T1E1) produced less rut damage than the other 11-axle trucks. It should be noted that the truck that has a quad axle (S1T2Q1) as a maximum axle group shows similar or slightly higher truck factor than the one with tandems and tridem (S1T2Tr2) because it has 3 single axles. For a more detailed discussion of this laboratory experiment, see (Salama, 2005).

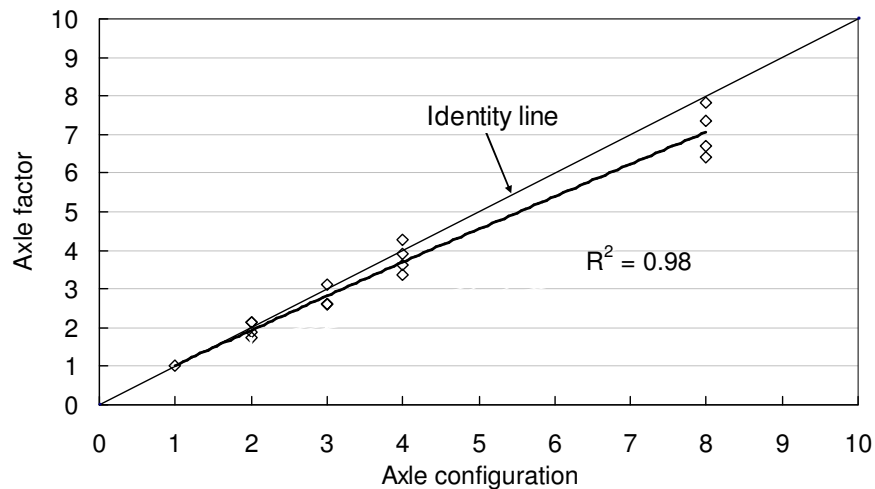


Figure 9. Axle factors for different axle configurations.

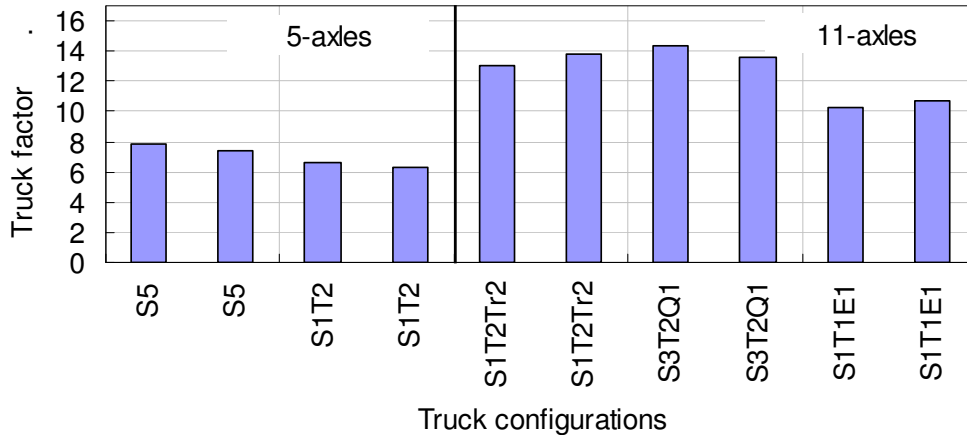


Figure 10. Truck factor for different truck configurations.

5 CONCLUSION

The results from mechanistic analyses showed that there is little to no interaction between axles in terms of vertical strains within the AC layer. For the vertical strains within the base layer, the interaction between axles increases with increasing AC layer thickness. On the other hand, there is always high interaction between axles in the subgrade layer vertical strain response. Despite the interaction between axles, the mechanistic analysis in this study indicates that the rutting damage is proportional to the number of axles within an axle group or truck. Laboratory results confirmed the near proportionality of rut damage for multiple axles. However, the same cannot be said for truck configurations, where the variable rest periods between axle groups appear to affect the cumulative rut damage differently.

6 REFERENCES

- Ali, H., S. D. Tayabji, and F. L. Torre, 1998. "Calibration of Mechanistic-Empirical Rutting Model for In-service Pavements," *Transportation Research Record*, No.1629, pp. 159-168.
- Ali, H. and S. D. Tayabji, 2000. "Using Transverse Profile Data to Compute Plastic Deformation Parameters for Asphalt Concrete Pavements," *Transportation Research Record*, No.1716, pp. 89-97.
- Claussen, A., J. M. Edwards, P. Sommer, and P. Uge, 1977. "Asphalt Pavement Design -The Shell Method," *Proceedings of 4th International Conference on the Structural Design of Asphalt Pavements*, pp. 39-74.
- Harichandran, R. S., Mahmood, T., Raab, A., and Baladi, G. Y., 1994 "Backcalculation of pavement layer moduli, thicknesses and bedrock depth using a modified Newton method." In *Nondestructive Testing of Pavements and Backcalculation of Moduli (Second Volume)*, ASTM STP 1198, H. L. Von Quintas, A. J. Bush and G. Y. Baladi (eds.) American Society for Testing and Materials, Philadelphia, PA, 68-82.
- Huang, Y. H., 2004. "Pavement Analysis and Design," Second edition, Prentice Hall.

- Moavenzadeh, F., J. E. Soussou, H. K. Findakly, and B. Brademeyer, 1974. "Synthesis for Rational Design of Flexible Pavements," FHWA Report FH 11-776.
- Salama, H., 2005. "Effect of heavy multiple axle trucks on flexible pavement rutting," Ph.D. Dissertation, Department of Civil and Environmental Engineering, Michigan State University, East Lansing, Michigan.
- Salama, H., K. Chatti and S. Haider, 2006. "Calibration of Mechanistic-Empirical Rutting Model Using In-service Pavement Data from the SPS-1 Experiment" Proceedings of the 85th Annual Meeting of the Transportation Research Board.
- Salama, H., K. Chatti and S. Haider, 2006. "Backcalculation of Permanent Deformation Parameters Using Time Series Rut Data from In-service Pavements in the LTPP SPS-1 Experiment," Proceedings of the 85th Annual Meeting of the Transportation Research Board.
- Shook, J., F. N. Finn, M. W. Witzak, and C. L. Monismith, 1982. "Thickness Design of Asphalt Pavement - The Asphalt Institute Method," Proceedings of 5th International Conference on the Structural Design of Asphalt Pavements, pp. 17-44.
- White, T., E. John, J. Adam, and F. Hongbing, 2002. "Contribution of Pavement Structural Layers to Rutting of Hot Mix Asphalt Pavements," NCHRP Report 468.
- Witzak, M. W., K. Kaloush, T. Pellinen, M. El-basyouny, and H. Von Quintus, 2002. "Simple Performance Test for Superpave Mix Design" NCHRP report 465, National Academy Press, Washington, D.C.
- Witzak, M.W. and M. El-Basyouny, 2004. "Calibration of Permanent Deformation Models for Flexible Pavements"; Appendix GG-1 of "Guide for Mechanistic-empirical Design of New and Rehabilitated Pavement Structures." ARA, Inc., ERES Division, 505 West University Avenue, Champaign, IL 61820.